

Different wave patterns for two-coupled Maccari's system with complex structure via truncated Painlevé approach

Hongcai Ma(马红彩), Xinru Qi(戚心茹), and Aiping Deng(邓爱平)
Citation: Chin. Phys. B, 2023, 32 (**12**): 120503. DOI: 10.1088/1674-1056/acf497
Journal homepage: http://cpb.iphy.ac.cn; http://iopscience.iop.org/cpb

What follows is a list of articles you may be interested in

Breather and its interaction with rogue wave of the coupled modified nonlinear Schrödinger equation

Ming Wang(王明), Tao Xu(徐涛), Guoliang He(何国亮), and Yu Tian(田雨)
Chin. Phys. B, 2023, 32 (**5**): 050503. DOI: 10.1088/1674-1056/ac833d

Deformed two-dimensional rogue waves in the (2+1)-dimensional Korteweg-de Vries equation

Yulei Cao(曹玉雷), Peng-Yan Hu(胡鹏彦), Yi Cheng(程艺), and Jingsong He(贺劲松)
Chin. Phys. B, 2021, 30 (**3**): 030503. DOI: 10.1088/1674-1056/abd15e

Lump, lumpoff and predictable rogue wave solutions to a dimensionally reduced Hirota bilinear equation

Haifeng Wang(王海峰), Yufeng Zhang(张玉峰)
Chin. Phys. B, 2020, 29 (**4**): 040501. DOI: 10.1088/1674-1056/ab75d7

Formation mechanism of asymmetric breather and rogue waves in pair-transition-coupled nonlinear Schrödinger equations

Zai-Dong Li(李再东), Yang-yang Wang(王洋洋), Peng-Bin He(贺鹏斌)
Chin. Phys. B, 2019, 28 (**1**): 010504. DOI: 10.1088/1674-1056/28/1/010504

Symmetry and asymmetry rogue waves in two-component coupled nonlinear Schrödinger equations

Zai-Dong Li(李再东), Cong-Zhe Huo(霍丛哲), Qiu-Yan Li(李秋艳), Peng-Bin He(贺鹏斌), Tian-Fu Xu(徐天赋)
Chin. Phys. B, 2018, 27 (**4**): 040505. DOI: 10.1088/1674-1056/27/4/040505

Different wave patterns for two-coupled Maccari's system with complex structure via truncated Painlevé approach

Hongcai Ma(马红彩)[†], Xinru Qi(戚心茹)[‡], and Aiping Deng(邓爱平)

Department of Applied Mathematics, Donghua University, Shanghai 201620, *China*

(Received 9 August 2023; revised manuscript received 27 August 2023; accepted manuscript online 29 August 2023)

We focused on the two-coupled Maccari's system. With the help of truncated Painlevé approach (TPA), we express local solution in the form of arbitrary functions. From the solution obtained, using its appropriate arbitrary functions, we have generated the rogue wave pattern solutions, rogue wave solutions, and lump solutions. In addition, by controlling the values of the parameters in the solutions, we show the dynamic behaviors of the rogue wave pattern solutions, rogue wave solutions, and lump solutions with the aid of Maple tool. The results of this study will contribute to the understanding of nonlinear wave dynamics in higher dimensional Maccari's systems.

Keywords: two-coupled Maccari's system, rogue wave, lump wave, truncated Painlevé approach

PACS: 05.45.Yv, 02.30.Ik, 47.20.Ky, 52.35.Mw **DOI:** 10.1088/1674-1056/acf497

1. Introduction

In recent years, the investigation of exact solution of nonlinear partial differential equations has become a hot issue in most scientific research fields, such as fluid dynamics, physics, chemistry, genetics, optical fibers, and mathematical biology. Through the continuous exploration and efforts of researchers, more and more methods for solving nonlinear evolution equations have been developed and promoted, such as extend Fan sub-equation mapping method,[1] Weierstrass semi-rational expansion method,[2] tensor method,[3] homotopy analysis method,[4] homogeneous balance method,[5] third-order newton-type method,[6] Laplace decomposition method,[7] Adomian decomposition method,[8] Newton-raphson method,[8] multipoint method,[9] Darboux transformation,[10] and TPA.[11] Through the above methods, many wave-like solutions can be constructed.

There are widespread concern about the existence of wave-like solutions in the ocean. At present, wave-like solutions have been mentioned by a large number of nonlinear systems, such as the Fokas–Lenells equation,[10] the $(2+1)$-dimensional Maccari's system,[12] the nonlinear Schrödinger equation,[13] and the $(3+1)$-dimensional variable-coefficient nonlinear wave equation.[14] There are many ways to get wave-like solutions. Thilakavathy *et al.* obtained the local solutions, such as multi-rogue wave solutions, rogue wave doublet solutions, and lump wave solutions by using TPA.[12] Ahmed *et al.* constructed the additional solutions to the Maccari system by Lie symmetry approach.[15] Jabbari *et al.* constructed exact solutions of the coupled Higgs equation and the Maccari system by the semi-inverse method and (G'/G)-expansion method.[16] The first integral method can be used to study the exact solutions of the Maccari's system, such as the coupled Maccari's system, two coupled nonlinear Maccari's system, three coupled nonlinear Maccari's system.[17] Two methods: the planar dynamic system method and the polynomial complete discriminant system method, are used to find the solutions of the coupled nonlinear Maccari systems.[18] It is obvious that the new exact solutions to the coupled nonlinear Maccari's system have complex structures by extended rational sine–cosine and rational sinh–cosh methods.[19]

When studying the Maccari equation, we have to mention its origin. It was derived by means of an extension of the reduction method[20] developed by Tang.[21] And it has the following form:

$$\begin{cases} \mathrm{i}A_t + A_{xx} + LA = 0, \\ \mathrm{i}B_t + B_{xx} + LB = 0, \\ L_y = (|A|^2 + |B|^2)_x. \end{cases} \tag{1}$$

The Maccari system is equivalent to the long-wave-short wave interaction model.[21] In addition, the Maccari system is also a special case of a generalized $(N+M)$-component $(2+1)$-dimensional AKNS system, from which the Maccari system can be obtained by simplification.[21,22] Inspired by the above article, this article is devoted to the study of the two-coupled Maccari's system[17,23–25]

$$\begin{cases} \mathrm{i}X_t + X_{xx} + RX = 0, \\ \mathrm{i}Y_t + Y_{xx} + RY = 0, \\ R_t + R_y + (|X+Y|^2)_x = 0, \end{cases} \tag{2}$$

where $\mathrm{i} = \sqrt{-1}$, $X(x,y,t)$ and $Y(x,y,t)$ are complex short wave amplitudes and $R(x,y,t)$ is real long wave amplitude. The subscripts denote partial differentiation and aster-

[†]Corresponding author. E-mail: hongcaima@hotmail.com
[‡]Corresponding author. E-mail: qixinrudhu@163.com

© 2023 Chinese Physical Society and IOP Publishing Ltd

isk means complex conjugate hereafter. From the above discussion, we can easily see that equations (1) and (2) are very similar in form, but the third equation is different. This is because their derived equations are different, although they are derived by the same reduction method.[20,23] In terms of expansion, equation (1) is derived from the Nizhnik equation,[20] while equation (2) is derived by considering the Kadomtsev–Petviashvili equation.[23] It is also important to note that both Eqs. (1) and (2) are integrable, which can be proved by deriving the corresponding Lax pairs.

At present, the development of the Maccari system has been matured, and many researchers have found many interesting properties. Abundant localized coherent structures are revealed by the variable separation approach, some special types of the localized excitations like the multiple solitoffs, dromions, lumps, ring solitons, breathers, and instantons are plotted also, and it is not difficult to find that the interaction between two traveling ring soliton solutions is completely elastic.[21,26] In contrast, we want to study wave forms that do not interact with each other. To do this, we use the TPA method to investigate Eq. (2). In this article, by choosing appropriate functions, we obtain rogue wave pattern solutions, rogue wave solutions, and lump wave solutions. It is worth mentioning that the rogue wave pattern we obtained is different from the traditional rogue wave. Compared to the traditional rogue wave, the rogue wave pattern we obtained is characterized by extreme suddenness, but it does not disappear. In other words, the rogue wave pattern has half the rogue wave property, half the lump solution property.

The layout of this paper is arranged as follows. In Section 2, we show how the two-coupled Maccari equation can be solved by TPA. In Section 3, we construct wave-like solutions by various arbitrary functions. Finally, in Section 4, we summarize this paper.

2. Solution of the two-coupled Maccari's system by TPA

In order to solve the above equation, we define $X = u$, $X^* = v$, $Y = m$, and $Y^* = n$, we rewrite Eq. (2) as follows:

$$\begin{cases} \mathrm{i}u_t + u_{xx} + Ru = 0, \\ -\mathrm{i}v_t + v_{xx} + Rv = 0, \\ \mathrm{i}m_t + m_{xx} + Rm = 0, \\ -\mathrm{i}n_t + n_{xx} + Rn = 0, \\ R_t + R_y + (|u+m|^2)_x = 0. \end{cases} \tag{3}$$

We can introduce a local Laurent expansion of the variables u, v, m, n, and R in neighborhood of a non-characteristic singular manifold $\phi(x,y,t) = 0$, $\phi_x \neq 0$, $\phi_y \neq 0$. To find out the solutions of the above two-coupled Maccari's system we consider the following transformation:

$$u = u_0\phi^{\alpha}, \quad v = v_0\phi^{\beta}, \quad m = m_0\phi^{\gamma}, \quad n = n_0\phi^{\delta}, \quad R = R_0\phi^{\eta}, \tag{4}$$

where u_0, v_0, m_0, n_0, and R_0 are analytic functions of (x,y,z) and α, β, γ, δ, and η are integers to be determined.

By inserting Eq. (4) into Eq. (3) and balancing the most dominant terms, we have

$$\alpha = \beta = \gamma = \delta = -1, \quad \eta = -2. \tag{5}$$

The Laurent series of the solutions of Eq. (3) at the constant level term yields the following Bäcklund transformation:

$$\begin{aligned} &u = \frac{u_0}{\phi} + u_1, \quad v = \frac{v_0}{\phi} + v_1, \quad m = \frac{m_0}{\phi} + m_1, \\ &n = \frac{n_0}{\phi} + n_1, \quad R = \frac{R_0}{\phi^2} + \frac{R_1}{\phi} + R_2. \end{aligned} \tag{6}$$

Assuming $u_1 = v_1 = m_1 = n_1 = 0, R = R_2(x,t)$. Substituting Eq. (6) and the above assumptions into Eq. (3) and proposing coefficients of $(\phi^{-3}, \phi^{-3}, \phi^{-3}, \phi^{-3}, \phi^{-3})$, we have

$$\begin{cases} 2u_0\phi_x^2 + R_0u_0 = 0, \\ 2v_0\phi_x^2 + R_0v_0 = 0, \\ 2m_0\phi_x^2 + R_0m_0 = 0, \\ 2n_0\phi_x^2 + R_0n_0 = 0, \\ -2R_0\phi_t - 2R_0\phi_y - 2\phi_x(u_0+m_0)(v_0+n_0) = 0. \end{cases} \tag{7}$$

By solving Eq. (7), we obtain

$$\begin{cases} 2\phi_x^2 + R_0 = 0, \\ R_0\phi_t + R_0\phi_y + \phi_x(u_0+m_0)(v_0+n_0) = 0. \end{cases} \tag{8}$$

Proposing coefficients of $(\phi^{-2}, \phi^{-2}, \phi^{-2}, \phi^{-2}, \phi^{-2})$, we obtain

$$\begin{cases} -\mathrm{i}u_0\phi_t - 2\phi_xu_{0x} - u_0\phi_{xx} + u_0R_1 = 0, \\ \mathrm{i}v_0\phi_t - 2\phi_xv_{0x} - v_0\phi_{xx} + v_0R_1 = 0, \\ -\mathrm{i}m_0\phi_t - 2\phi_xm_{0x} - m_0\phi_{xx} + m_0R_1 = 0, \\ \mathrm{i}n_0\phi_t - 2\phi_xn_{0x} - n_0\phi_{xx} + n_0R_1 = 0, \\ R_{0t} - R_1\phi_t + R_{0y} - R_1\phi_y \\ \quad + (u_{0x}+m_{0x})(v_0+n_0) + (u_0+m_0)(v_{0x}+n_{0x}) = 0. \end{cases} \tag{9}$$

Substituting Eq. (8) into the last equation of Eq. (9), yields the following form:

$$R_1 = 2\phi_{xx} - \frac{2\phi_x(\phi_t+\phi_y)_x}{\phi_t+\phi_y}. \tag{10}$$

Substituting Eq. (10) into Eq. (9), the variable u_0, v_0, m_0, and n_0 can be solved as follows:

$$\begin{cases} u_0 = S_1(y)\exp\left[\int \left(\frac{-\mathrm{i}\phi_t+\phi_{xx}}{2\phi_x} - \frac{(\phi_t+\phi_y)_x}{\phi_t+\phi_y}\right)\mathrm{d}x\right], \\ v_0 = S_1(y)\exp\left[\int \left(\frac{\mathrm{i}\phi_t+\phi_{xx}}{2\phi_x} - \frac{(\phi_t+\phi_y)_x}{\phi_t+\phi_y}\right)\mathrm{d}x\right], \\ m_0 = S_2(y)\exp\left[\int \left(\frac{-\mathrm{i}\phi_t+\phi_{xx}}{2\phi_x} - \frac{(\phi_t+\phi_y)_x}{\phi_t+\phi_y}\right)\mathrm{d}x\right], \\ n_0 = S_2(y)\exp\left[\int \left(\frac{\mathrm{i}\phi_t+\phi_{xx}}{2\phi_x} - \frac{(\phi_t+\phi_y)_x}{\phi_t+\phi_y}\right)\mathrm{d}x\right], \end{cases} \tag{11}$$

where $S_1(y)$ and $S_2(y)$ are low-dimensional arbitrary functions with respect to y.

By proposing coefficients of $(\phi^{-1},\phi^{-1},\phi^{-1},\phi^{-1},\phi^{-1})$, we have

$$\begin{cases} \mathrm{i}u_{0t}+u_{0xx}+u_0R_2=0, \\ -\mathrm{i}v_{0t}+v_{0xx}+v_0R_2=0, \\ \mathrm{i}m_{0t}+m_{0xx}+m_0R_2=0, \\ -\mathrm{i}n_{0t}+n_{0xx}+n_0R_2=0, \\ R_{1t}+R_{1y}=0. \end{cases} \tag{12}$$

Substituting Eq. (10) into the last equation of Eq. (12) yields the following trilinear form:

$$\begin{aligned} &2\phi_{xxt}(\phi_t+\phi_y)^2-2\phi_{xt}(\phi_t+\phi_y)_x(\phi_t+\phi_y) \\ &+2\phi_x(\phi_t+\phi_y)_x(\phi_t+\phi_y)_t \\ &-2\phi_x(\phi_t+\phi_y)_{xt}(\phi_x+\phi_y)+2\phi_{xxy}(\phi_t+\phi_y)^2 \\ &-2\phi_{xy}(\phi_t+\phi_y)_x(\phi_t+\phi_y) \\ &-2\phi_x(\phi_t+\phi_y)_{xy}(\phi_x+\phi_y) \\ &+2\phi_x(\phi_t+\phi_y)_x(\phi_t+\phi_y)_y=0. \end{aligned} \tag{13}$$

The above trilinear Eq. (13) makes it clear that any manifold $\phi(x,t)$ can be partitioned into the following form:

$$\phi=\phi_1(x)+\phi_2(t), \tag{14}$$

where $\phi_1(x)$ and $\phi_2(t)$ are the arbitrary functions. Substituting Eqs. (11) and (14) into the second expression of Eq. (8) yields the following condition:

$$S_2(y)=-S_1(y)\pm\sqrt{2\phi_{2t}}. \tag{15}$$

Once again, proposing coefficients of $(\phi^0,\phi^0,\phi^0,\phi^0,\phi^0)$, we have

$$R_{2t}+R_{2y}=0. \tag{16}$$

Substituting Eq. (14) into Eq. (11), and with the help of Eq. (16), R_2 is obtained in the following form:

$$R_2=-\int\frac{\phi_{2tt}}{2\phi_{1x}}\,\mathrm{d}x+\frac{\phi_{2t}^2+\phi_{1xx}^2-2\phi_{1x}\phi_{1xxx}}{4\phi_{1x}^2}. \tag{17}$$

By substituting the first equation of Eqs. (8), (10), (11), (14), and (17) into Eq. (6), the solution of the two-coupled Maccari's system is obtained as follows:

$$\begin{aligned} X&=\frac{S_1(y)\exp[\int(\frac{-\mathrm{i}\phi_{2t}+\phi_{1xx}}{2\phi_{1x}})\,\mathrm{d}x]}{\phi_1(x)+\phi_2(t)}, \\ Y&=\frac{S_2(y)\exp[\int(\frac{-\mathrm{i}\phi_{2t}+\phi_{1xx}}{2\phi_{1x}})\,\mathrm{d}x]}{\phi_1(x)+\phi_2(t)}, \\ R&=\frac{-2\phi_{1x}^2}{(\phi_1(x)+\phi_2(t))^2}+\frac{2\phi_{1xx}}{\phi_1(x)+\phi_2(t)} \\ &\quad-\int\frac{\phi_{2tt}}{2\phi_{1x}}\,\mathrm{d}x+\frac{\phi_{2t}^2+\phi_{1xx}^2-2\phi_{1x}\phi_{1xxx}}{4\phi_{1x}^2}. \end{aligned} \tag{18}$$

The squared forms of the first two equations of Eq. (18) are as follows:

$$|X|^2=\frac{S_1^2(y)\phi_{1x}}{(\phi_1(x)+\phi_2(t))^2}. \tag{19}$$

When $S_2(y)=-S_1(y)-\sqrt{2\phi_{2t}}$,

$$|Y|^2=\frac{(-S_1(y)-\sqrt{2\phi_{2t}})^2\phi_{1x}}{(\phi_1(x)+\phi_2(t))^2}. \tag{20}$$

When $S_2(y)=-S_1(y)+\sqrt{2\phi_{2t}}$,

$$|Y|^2=\frac{(-S_1(y)+\sqrt{2\phi_{2t}})^2\phi_{1x}}{(\phi_1(x)+\phi_2(t))^2}. \tag{21}$$

3. Localized solutions of the two-coupled Maccari's system

3.1. Rogue wave pattern solution

In the following, we verify the effect of parameter values on the rogue wave. To draw the graph, we choose any of the following functional forms from Eqs. (19)–(21). Figures 1–3 show the wave patterns

$$\begin{aligned} \phi_1(x)&=\frac{b_1x}{a(\alpha(x-2)^2+1)}, \\ \phi_2(t)&=\frac{1}{c\gamma^2(t-2)^2}, \\ S_1(y)&=\frac{d_1}{b(y-2)^2}. \end{aligned}$$

In Fig. 1, time has a great influence on the amplitude of waves. When $t=-1$ and $t=5$, the amplitude of the wave is the largest. When $t=0$ and $t=4$, the amplitude of the wave decreases. Moreover, we can see from Fig. 1 that the positions of the wave do not change with time.

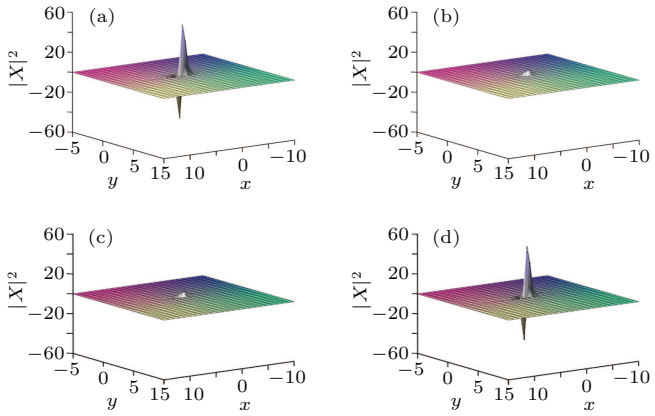


Fig. 1. The rogue pattern of Eq. (19) by taking $c=-8.5$, $\gamma=0.7$, $b_1=0.22$, $a=30$, $\alpha=1.22$, $d_1=1.5$, and $b=100$, for (a) $t=-1$, (b) $t=0$, (c) $t=4$, and (d) $t=5$.

In Fig. 2, there are two kinds of fluctuations, one is the overall fluctuation, and the other is the local fluctuation. These two fluctuations have the same variation over time. When

$t = 15$, the amplitude of the wave is the smallest. When $t = 20$, the amplitude begins to increase. When $t = 25$, the amplitude continues to decrease and the amplitude of the wave is the largest at $t = 30$.

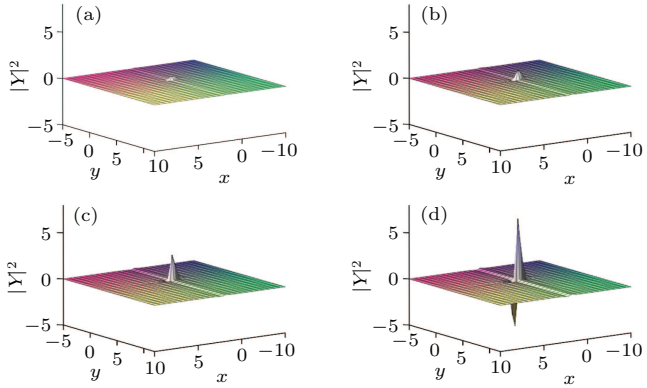


Fig. 2. The rogue pattern of Eq. (20) by taking $S_2(y) = -S_1(y) - \sqrt{2\phi_{2t}}$, $c = -9.5$, $\gamma = 0.02$, $b_1 = 0.09$, $a = 2$, $\alpha = 5$, $d_1 = 1$, $b = 90$, for different time: $t = 15$ (a), $t = 20$ (b), $t = 25$ (c), and $t = 30$ (d).

In Fig. 3, by fixing the appropriate values of parameters, we obtained the corresponding wave solutions.

When $t = 10$, the amplitude of the wave is the smallest. When $t = 15$, the amplitude begins to increase. When $t = 20$, the amplitude of the fluctuation continues to increase. When $t = 25$, the amplitude of the wave is the largest.

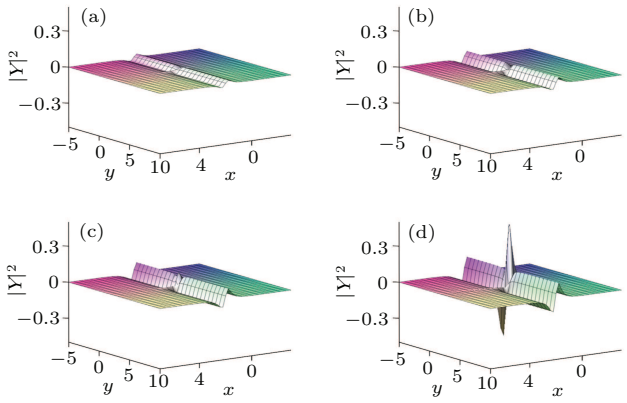


Fig. 3. The rogue pattern of Eq. (21) by taking $S_2(y) = -S_1(y) + \sqrt{2\phi_{2t}}$, $c = -9.5$, $\gamma = 0.025$, $b_1 = 0.09$, $a = 2$, $\alpha = 5$, $d_1 = 1$, $b = 90$, for different time: $t = 10$ (a), $t = 15$ (b), $t = 20$ (c), and $t = 25$ (d).

3.2. Rogue wave solution

In this subsection, in order to get a more complete rogue wave characteristics, we re-select the functions $\phi_1(x)$, $\phi_2(t)$, and $S_1(y)$, and give the corresponding wave solutions, as shown in Figs. 4–6.

$$\phi_1(x) = \frac{cb_1}{(1+\alpha x^2)} + \frac{x}{(2(x-4)^2+1)^2},$$
$$\phi_2(t) = \frac{cb_1}{(1+2(t-4))^2},$$
$$S_1(y) = \frac{4\gamma^2}{y^2+3}.$$

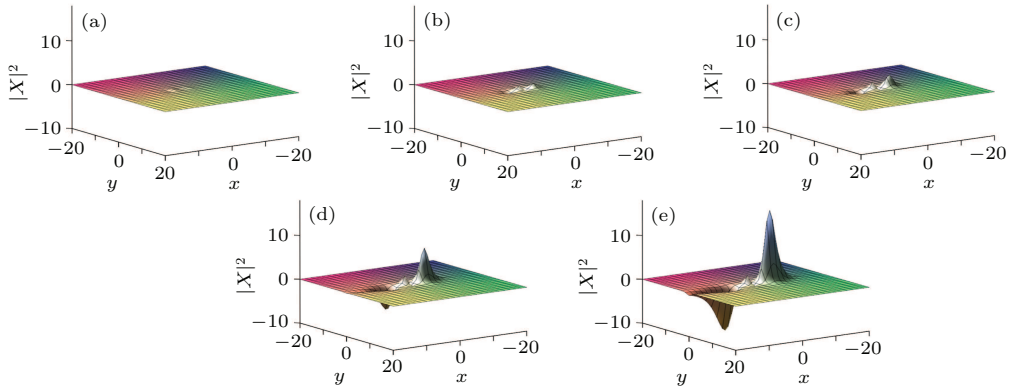


Fig. 4. The rogue pattern of Eq. (19) by taking $\alpha = 1.2$, $\gamma = 0.5$, $b_1 = 1.2$, $c = 1$, for different time: $t = 2.5$ (a), $t = 1$ (b), $t = -1$ (c), $t = -5$ (d), $t = -10$ (e).

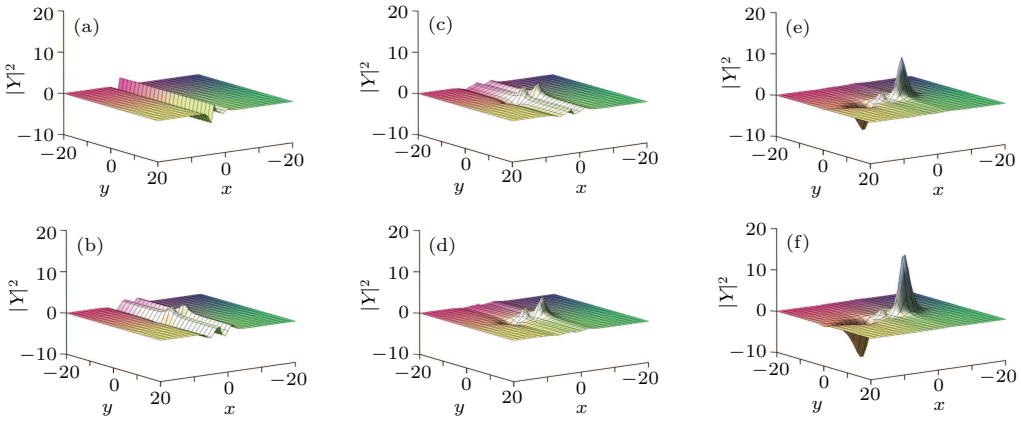


Fig. 5. The rogue pattern of Eq. (20) by taking $S_2(y) = -S_1(y) - \sqrt{2\phi_{2t}}$, $\alpha = 1.2$, $\gamma = 0.5$, $b_1 = 1.2$, $c = 1$, for different time: $t = 3.45$ (a), $t = 2$ (b), $t = 1$ (c), $t = -1$ (d), $t = -5$ (e), $t = -8$ (f).

In Fig. 4, it is not difficult to find that the amplitude of the waves is related to time. With the increase of time, the fluctuation range decreases. The amplitude of the waves is maximum at $t = -10$, then decreases with increasing time and finally disappears at $t = 2.5$.

In Fig. 5, there are very interesting waves. There are two different kinds of waves, one is the overall fluctuation, and the other is the local fluctuation. No matter what kind of wave, its fluctuation amplitude is related to time. An overall fluctuating wave whose amplitude decreases with time and finally disappears at $t = -8$. The amplitude of the local wave decreases with time and finally disappears at $t = 3.45$.

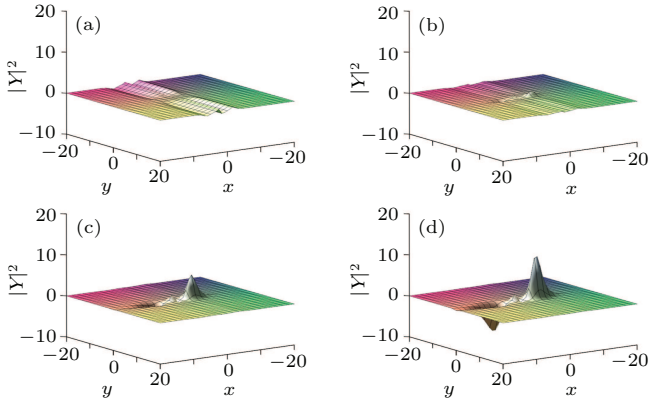


Fig. 6. The rogue pattern of Eq. (21) by taking $S_2(y) = -S_1(y) + \sqrt{2\phi_{2t}}$, $\alpha = 1.2$, $\gamma = 0.5$, $b_1 = 1.2$, $c = 1$, for different time: $t = 1$ (a), $t = -1$ (b), $t = -5$ (c), $t = -8$ (d).

In Fig. 6, we can see that there are two different kinds of fluctuations, one local fluctuation and the other overall fluctuation. A locally fluctuating wave whose amplitude decreases with time and vanishes at $t = 1$. The amplitude of the overall wave decreases with time and disappears at $t = -8$.

3.3. Lump wave solution

In this part, in order to verify the existence of the lump wave, we assign the following arbitrary function forms to the functions $\phi_1(x)$, $\phi_2(t)$, $S_1(y)$ in Eqs. (19)–(21) and obtain the graphs shown in Figs. 7–9.

$$\phi_1(x) = \frac{b_1}{(a^2x^2+1)+1},$$
$$\phi_2(t) = \frac{b_2}{(b^2t^2+1)+1},$$
$$S_1(y) = \frac{b_3}{(c^2y^2+1)+1}.$$

In Fig. 7, we can find that the amplitude of the wave at $t = 0$ is very small, close to stability. When $t = 3$, the fluctuation amplitude begins to increase. When $t = 5$, the fluctuation amplitude is the largest. When time changes, the position of the lump wave does not change, but the width of the wave becomes wider as time increases.

In Fig. 8, it can be observed from the figure that the change of time has a great influence on the amplitude of the wave. When $t = 5$, the amplitude of the wave is the smallest, and when $t = 10$, the amplitude is the largest, and compared with the amplitude when $t = 5$, the increase of the amplitude at $t = 10$ is very obvious.

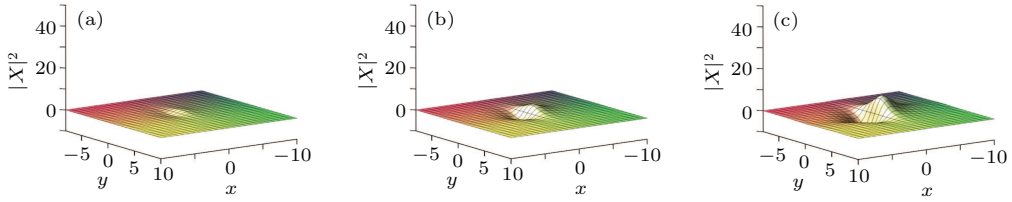


Fig. 7. The lump wave pattern of Eq. (19) by taking $b_1 = 7$, $b_2 = 25$, $b_3 = 25$, $a = 0.9$, $b = 0.5$, $c = 0.5$, $\gamma = 0.5$, for different time: $t = 0$ (a), $t = 3$ (b), $t = 5$ (c).

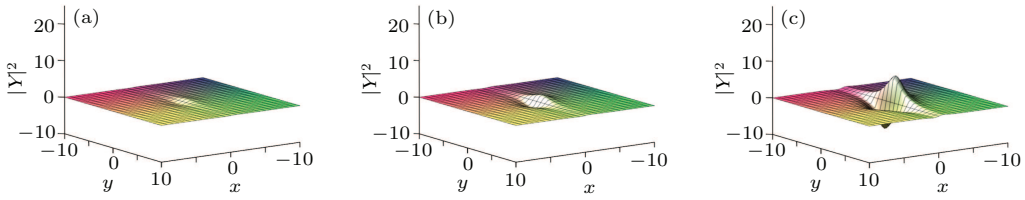


Fig. 8. The lump wave pattern of Eq. (19) by taking $S_2(y) = -S_1(y) - \sqrt{2\phi_{2t}}$, $b_1 = 7$, $b_2 = -250$, $b_3 = 25$, $a = 0.9$, $b = 0.5$, $c = 0.5$, $\gamma = 0.5$, for different time: $t = 5$ (a), $t = 7$ (b), $t = 10$ (c).

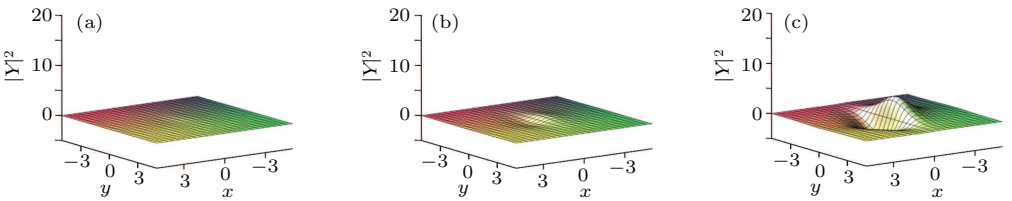


Fig. 9. The lump wave pattern of Eq. (19) by taking $S_2(y) = -S_1(y) + \sqrt{2\phi_{2t}}$, $b_1 = 7$, $b_2 = -250$, $b_3 = 25$, $a = 0.9$, $b = 0.5$, $c = 0.5$, $\gamma = 0.5$, for different time $t = 5$ (a), $t = 7$ (b), $t = 10$ (c).

In Fig. 9, it can be seen from the figure that when $t = 5$, the amplitude of the wave is extremely weak and gradually disappears, when $t = 7$, the amplitude of the wave fluctuates weakly, and when $t = 10$, the amplitude changes greatly.

4. Conclusion

In this paper, we solved the $(2+1)$-dimensional nonlinear two-coupled Maccari equation by using TPA and obtained its solutions. By choosing three arbitrary functions $\phi_1(x)$, $\phi_2(t)$, and $S_1(y)$ in Eqs. (19), (20), and (21), the localized solutions such as rogue wave pattern solution, rogue wave solution, and lump wave solution are obtained. The rogue wave pattern solution is shown in Figs. 1–3. The position of the image of the rogue wave pattern solution does not change with time. But the amplitude of the rogue wave pattern solution is affected by time. It is worth mentioning that the rogue wave pattern solution we obtained is not the traditional rogue wave solution, the wave solution we get did not disappear in the end. In other words, it has half the rogue wave property, half the lump solution property. The rogue wave solution is constructed and shown in Figs. 4–6. The amplitude of this wave solution is affected by time, and different time corresponds to different amplitudes of fluctuations. The most important thing is that at some points, the wave will eventually disappear. The lump wave solution is shown in Figs. 7–9. The change of time affects the width of the lump wave, and the width of the lump wave increases with time. In this context, the solution of the $(2+1)$-dimensional nonlinear two-coupled Maccari equation formed deserves further investigation. With Eq. (2), we obtained rogue wave pattern solution, rogue wave solution, and lump wave solution. We hope that in the future research work, more methods will be proposed to gain more new solutions.

References

[1] Cheemaa N and Younis M 2016 *Nonlinear Dyn.* **83** 1395
[2] Chen Y and Yan Z Y 2006 *Appl. Math. Comput.* **177** 85
[3] Schnabel R B and Frank P D 1984 *Siam J. Numer. Anal.* **21** 815
[4] Abbasbandy S 2006 *Phys. Lett. A* **360** 109
[5] Wang M L, Zhou Y B and Li Z B 1996 *Phys. Lett. A* **216** 67
[6] Darvishi M T and Barati A 2007 *Appl. Math. Comput.* **187** 630
[7] Khan Y 2009 *Int. J. Nonlinear Sci. Num. Simul.* **10** 1373
[8] Abbasbandy S 2003 *Appl. Math. Comput.* **145** 887
[9] Petković M S, Neta B, Petković L D and Džunić J 2014 *Appl. Math. Comput.* **226** 635
[10] He J S, Xu S W and Porsezian K 2012 *J. Phys. Soc. Jpn.* **81** 124007
[11] Radha R, Tang X Y and Lou S Y 2007 *Z. Naturforsch. A* **62** 107
[12] Thilakavathy J, Amrutha R, Subramanian K and Rajan M M 2022 *Nonlinear Dyn.* **108** 445
[13] Akhmediev N, Ankiewicz A and Soto-Crespo J M 2009 *Phys. Rev. E* **80** 026601
[14] Liu J G and Zhu W H 2021 *Nonlinear Dyn.* **103** 1841
[15] Ahmed B S, Biswas A, Krishnan E and Kumar S 2013 *Rom. Rep. Phys.* **65** 1138
[16] Jabbari A, Kheiri H and Bekir A 2011 *Comput. Math. Appl.* **62** 2177
[17] Rostamy D and Zabihi F 2012 *Nonlinear Stud.* **19** 229
[18] Li Z, Xie X Y and Jin C J 2022 *Results Phys.* **41** 105932
[19] Vahidi J, Zekavatmand S M, Rezazadeh H, Inc M, Akinlar M A and Chu Y M 2021 *Results Phys.* **21** 103801
[20] Maccari A 1997 *J. Math. Phys.* **38** 4151
[21] Tang X Y, Lou S Y and Zhang Y 2002 *Phys. Rev. E* **66** 046601
[22] Lou S Y and Hu X B 1997 *J. Math. Phys.* **38** 6401
[23] Maccari A 1996 *J. Math. Phys.* **37** 6207
[24] Cheemaa N, Chen S and Seadawy A R 2020 *Results Phys.* **17** 102987
[25] İnç M, Aliyu A I, Yusuf A, Baleanu D and Nuray E 2018 *Mod. Phys. Lett. B* **32** 1850014
[26] Lou S Y, Chen C L and Tang X Y 2002 *J. Math. Phys.* **43** 4078